Highly efficient *Spirulina*-based bio-sorbent for removal of wastewater micropollutants

Marta Pedrosa[1,2,*], Rui S. Ribeiro[1,2], Sonia Guerra-Rodríguez[3,*], Jorge Rodríguez-Chueca[3], Encarnación Rodríguez[3], Adrián M.T. Silva[1,2], Maja Đolic[4,*], Ana Rita Lado Ribeiro[1,2]

[1]*Laboratory of Separation and Reaction Engineering - Laboratory of Catalysis and Materials (LSRE-LCM), Faculdade de Engenharia, Universidade do Porto, Rua Dr. Roberto Frias, 4200-465 Porto, Portugal*

[2]*ALiCE – Associate Laboratory in Chemical Engineering, Faculdade de Engenharia, Universidade do Porto, Rua Dr. Roberto Frias, 4200-465 Porto, Portugal*

[3]*Department of Industrial Chemical & Environmental Engineering, Escuela Técnica Superior de Ingenieros Industriales, Universidad Politécnica de Madrid, c/ José Gutiérrez Abascal 2, 28006, Madrid, Spain*

[4] *Faculty of Technology and Metallurgy, University of Belgrade, Karnegijeva 4, 11000, Belgrade, Serbia*

*Corresponding authors: Marta Pedrosa (up201409963@fe.up.pt); Sonia Guerra-Rodríguez (sonia.guerra@upm.es); Maja Đolic (mdjolic@tmf.bg.ac.rs)

This article has been accepted for publication and undergone full peer review.
Please cite this article as DOI: 10.1016/j.enmm.2022.100720

Abstract

This study proposes an efficient activated spirulina-based carbon material ($ASBCM_{800}$) with an extremely high specific surface area (2211 $m^2 g^{-1}$) to eliminate a wide range of micropollutants (MPs) frequently detected in wastewaters. This bio-sorbent can be simply synthesized by pre-carbonization at 600 °C, followed by activation/carbonization with KOH at 800 °C. The material was fully characterized by nitrogen adsorption-desorption isotherms, thermogravimetric analysis (TGA), attenuated total reflection Fourier transformed infrared (FTIR-ATR) spectroscopy, scanning (SEM) and transmission (TEM) electron microscopy, and X-ray photoelectron spectroscopy (XPS).

The highly porous bio-based $ASBCM_{800}$ material was tested as bio-sorbent of two model MPs – metoprolol (p*K*a 9.6) and diclofenac (p*K*a 4.0) – showing adsorption capacities of 660.5 and 588.9 mg g^{-1} at 25 °C, respectively, as determined by using the 3-parameter Sips model. In subsequent experiments, the novel bio-sorbent was also efficient to remove in less than 30 min more than 88% of most of 20 MPs belonging to 5 classes (6 antibiotics, 3 beta-blockers, 5 multi-class pharmaceuticals, 4 herbicides, and 2 insecticides) that were spiked at 100 μg L^{-1} each in secondary effluent of an urban wastewater treatment plant. This interesting strategy to remove trace MPs from complex matrices as wastewaters, will also contribute to control algal blooms and to mitigate eutrophication due to resource recovery of spirulina.

Keywords: *Spirulina* microalgae; adsorption; bio-based adsorbents; wastewater treatment; micropollutants.

1. Introduction

Water pollution is a worldwide environmental concern. The deterioration of water quality is caused by the continuous release of a wide range of contaminants into the aquatic environment. In fact, many types of pollutants are often detected in various water matrices including wastewater, surface water, groundwater, seawater, and even drinking water. These pollutants include dyes, heavy metals, and the so-called micropollutants (MPs) that comprise natural and synthetic substances typically found at trace levels, between ng L^{-1} and μg L^{-1}. Even at residual concentrations, organic MPs might lead to acute and/or chronic negative impacts on aquatic ecosystems and human health [1]. Therefore, urgent mitigation strategies to remove hazardous pollutants are needed to protect aquatic ecosystems and ultimately the human health from the potential exposure, bioaccumulation and/or biomagnification through the food chain, while avoiding the possible development of drug-resistance genes and microorganisms.

Depending on the type of water and contaminants to be removed, several treatment options have been suggested, including: (i) advanced oxidation processes (AOPs, conceptually based on the formation of hydroxyl radicals) or technologies (AOTs, a broader concept involving other types of radicals; (ii) membrane separation processes; (iii) biological treatments; and (iv) adsorption [2]. Despite their advantageous high efficiency in short time, oxidation processes have some drawbacks, such as the formation of reaction by-products that can often be more harmful than the original target compound, the potential high demand for chemicals (*e.g.*, in Fenton, persulfate activation, wet peroxide oxidation) and/or energy (*e.g.*, in ozonation, sonication, photocatalysis with artificial light) [3]. In the case of membrane separation technology, highly polluted waters can easily lead to severe membrane fouling, presenting high initial investment and energy requirements [4]. On the other hand, biological methods are slow and complex, requiring a strict maintenance to keep a microbial favorable environment, with low biodegradability of certain molecules [4]. Over the last decades, adsorption has gained importance as an efficient process to detoxify, purify, decolorize, deodorize, separate, and concentrate (for further removal or recovery) substances; or particularly as tertiary polishing treatment in urban wastewater treatment plants (UWWTPs) for the specific removal of MPs and reaction by-products. Its high efficiency coupled with the technological simplicity, easy operation, and economical feasibility, renders adsorption as an interesting decontamination process [5]. Activated carbons, activated alumina, organic polymeric resins, and zeolites are some examples of effective adsorbents, but in the last few decades other non-conventional materials have been suggested as more economic, efficient, and sustainable adsorbents for pollution control [5].

Certain sorbents of natural biological origin, such as bacteria, fungi, yeast, and algae, can possess advanced adsorptive properties and thus, bio-sorbents may be a promising solution to decrease the concentration of water pollutants in various matrices. In particular, microalgae have been attracting attention in the field of food supplements, pharmaceuticals, cosmetics, photosynthetic CO_2 capture, bioremediation, and biodiesel production [6-8]. These microalgae or its derivatives (*e.g.*, carbon-based adsorbents using microalgae as a starting material) can be used as an effective option for water treatment [9], while simultaneously mitigating eutrophication when these microalgae are collected from water bodies facing algal blooms. Furthermore, carbon-based adsorbents can also be obtained from microalgae residues that would be discarded after extraction of their lipids for biodiesel production, in line with the principle of residue upcycling, and circular economy, using cost-effective precursors and processes [6, 7, 10, 11].

Arthrospira platensis (hereafter referred to as spirulina) is a planktonic cyanobacterium composed of individual cells with diameter of ca. 8 µm, which grows in alkaline lakes at approximately 35 °C [12]. These blue-green filamentous microalgae are used as a nutritional supplement due to its high content of proteins, carbohydrates, lipids, phycobiliproteins, carotenoids, vitamins, and minerals [13]. Spirulina or its derivatives have been applied in the adsorption of metals [10, 14-33], dyes [6, 34-42], phenol [43], and antibiotics [7]. To the best of the authors' knowledge, the use of spirulina-based carbon materials to remove a wide range of MPs from urban wastewater samples has not been reported in the literature yet. Thus, the main goals of this work were to: (i) synthesize an activated spirulina-based carbon material ($ASBCM_{800}$) with high porosity and excellent adsorption features; (ii) understand its adsorption performance towards 2 target MPs with distinct p*K*a (ca. 9.6 for metoprolol and ca. 4.0 for diclofenac); and (iii) evaluate its efficiency for the simultaneous removal of 20 MPs (spiked each at 100 µg L^{-1}) from a secondary effluent of an UWWTP.

2. Materials and Methods

2.1. Chemicals

Commercially available spirulina extract (*Arthrospira platensis*) was purchased from Celeiro© (Lisboa, Portugal), with the following biochemical composition of microalgae per 100 g of dry weight: Fe (83.2 mg), Ca (332.5 mg), K (1040 mg), NaCl (0.9 g), proteins (65.9 g, which are composed by N, C, O and H), vitamin B12 (34 µg), vitamin E (12.7 mg), vitamin B6 (18.5 mg), fiber (5.1 g), carbohydrates (13.1 g), and lipids (1 g). Potassium hydroxide (KOH, 85 wt.%) was acquired from Jose Manuel Gomes dos Santos (JMGS, Odivelas, Potugal) and formic acid (99 wt.%) was obtained from Merck (Darmstadt, Germany). Acetonitrile (HPLC and MS grades) was purchased to VWR International (Fontenay-sous-Bois, France).

The following MP reference standards (>98 wt.%) were acquired from Sigma-Aldrich (Steinhein, Germany): alachlor, atenolol, atrazine, carbamazepine, ciprofloxacin hydrochloride, enrofloxacin, erythromycin, furosemide, isoproturon, metoprolol tartrate, ofloxacin, propranolol hydrochloride, simazine, tetracycline hydrochloride, thiacloprid, thiamethoxam, tramadol hydrochloride, trimethoprim, and warfarin. Diclofenac sodium salt was purchased from Cayman Chemical Company (Michigan, USA).

Metoprolol and diclofenac solutions were prepared by dissolution in ultrapure water supplied by a Milli-Q® water system (resistivity less than 18 MΩ cm^{-1}). A solution containing the 20 MPs at 100 mg L^{-1} was prepared in ethanol.

2.2. Synthesis of ASBCM$_{800}$

The 2-step synthesis of ASBCM$_{800}$ consisted in a pre-carbonization at 600 °C, followed by activation/carbonization with KOH at 800 °C. Firstly, ca. 3.3 g of commercial spirulina (*Arthrospira platensis*) biomass was pre-carbonized under a N_2 atmosphere (100 cm^3 min^{-1}) in a vertical furnace, set at 120, 400 and 600 °C, for 1 h at each temperature, with a heating ramp of 2 °C min^{-1}. Once cooled to room temperature, the resulting material was ground and sieved (particle diameter size in the range 0.1 - 0.25 mm), resulting in the material denoted as spirulina-based carbon material (SBCM$_{600}$). Afterwards, SBCM$_{600}$ was added to an aqueous solution of KOH (mass ratio of carbon material to KOH of 1:2), which was prepared by dissolution of KOH in 10 mL of water in an ice-bath. After impregnation with KOH overnight at room temperature, the suspension was dried at 80 ºC in an oven to evaporate the remaining water. The dried material was then annealed under N_2 atmosphere (100 cm^3 min^{-1}) in a vertical furnace, at 800 °C for 1 h, after a heating ramp of 2 °C min^{-1}. The activated material was washed with distilled water until the neutrality of the rinsing water was achieved, and dried at 80 °C in an oven, resulting in the ASBCM$_{800}$ material. For comparison purposes, an additional spirulina-based carbon material was prepared following the same protocol, except the activation step with KOH. Accordingly, the spirulina biomass was carbonized under a N_2 atmosphere (100 cm^3 min^{-1}) in a vertical furnace, at 120, 400, 600, and 800 °C, for 1 h at each temperature, with a heating ramp of 2 °C min^{-1}, resulting in the SBCM$_{800}$ material.

2.3. Characterization techniques

The textural properties, namely specific surface area (S_{BET}), non-microporous specific surface area (S_{meso}), micropore volume (V_{micro}), and total pore volume (V_{total}), were determined from N_2 adsorption-desorption isotherms at −196 °C, as described elsewhere [44]. The pH at the point of zero charge (pH$_{PZC}$) was determined based on previous studies [45, 46]. Briefly, the pH of 5 mL of 0.01 mol L^{-1} NaCl was adjusted with solutions of 0.1 mol L^{-1} HCl or 0.005 mol L^{-1} NaOH, following the addition of 15 mg of sample. After 24 h under stirring in an orbital shaking bath (type 462-0355 VWR international, Belgium) at 25 °C, the final pH was measured. The pH_{PZC} was calculated by the interception between the curve and the straight-line drawn in the graph final pH vs. initial pH.

Attenuated total reflection Fourier transformed infrared (FTIR-ATR) spectra were obtained in a JASCO spectrometer (FT/IR-6800), equipped with a ZeSn ATR crystal. Thermogravimetric analysis (TGA) was performed with a STA490 PC/4/H Luxx Netzsch equipment. The samples were heated from 50 to 900 ºC, at 10 ºC min^{-1} under air or N_2 atmosphere.

Scanning electron microscopy (SEM) images were obtained using a FEI Quanta 400 FEG ESEM/EDAX Genesis X4M instrument equipped with an energy dispersive spectrometer (EDS). SEM images were collected in secondary electron (SE) and backscattered electron detector (BSED) modes. Spirulina sample was coated with an Au/Pd thin film for 100 s and with a 15 mA current, by sputtering, using the SPI Module Sputter Coater equipment. Transmission electron microscopy (TEM) was performed using a JEOL JEM-2100 LaB6 instrument operated at 200 kV. TEM images were acquired with a Gatan Orius CCD camera at 2×binning.

X-ray photoelectron spectroscopy (XPS) analysis was performed using a SPECS system with XP50M X-ray source for Focus 500 and PHOIBOS 100/150 analyzer, and AlKα source (1486.74 eV) at a 12.5 kV and 32 mA. Survey spectra (0–1000 eV binding energy) were recorded with constant pass energy of 40 eV, step size 0.5 eV and dwell time of 0.2 s in the FAT mode. Detailed spectra of C 1s, O 1s, Ti 2p, Si 2p and Ru 3d peaks were recorded with constant pass energy of 20 eV, step size of 0.1 eV, and dwell time of 2 s in the FAT mode. Spectra were obtained at a pressure of 9×10^{-9} mbar. To minimize effects of charging at the samples, a SPECS FG15/40 electron flood gun was used for charge neutralization. All the peak positions were referenced to C1s at 284.8 eV. Spectra were collected by a SpecsLab data analysis software supplied by the manufacturer and analyzed with commercial CasaXPS software package.

2.4. Kinetic and equilibrium adsorption experiments

Adsorption kinetic tests were performed in amber glass flasks filled with 50 mL of individual solutions containing 1 mg L^{-1} of either metoprolol or diclofenac and 0.25 g L^{-1} of $ASBCM_{800}$, which were kept at 25 °C under stirring for 3 h.

Adsorption equilibrium tests were performed in amber glass flasks filled with 10 mL of individual solutions containing either metoprolol or diclofenac (with varying initial concentrations) and 0.25 g L^{-1} of $ASBCM_{800}$, which were kept in an orbital shaking bath at 25 °C, for 5 days, until equilibrium was reached. Non-linearized regression (Langmuir, Freundlich, Sips, and Redlich-Peterson models) was performed with the OriginLab software.

Langmuir (Eq. (1)), Freundlich (Eq. (2)), Sips (Eq. (3)) and Redlich-Peterson (Eq. (4)) models were used to fit the experimental adsorption isotherms data for diclofenac and metoprolol.

$$q_e = \frac{q_{sat}.b.C_e}{1+b.C_e} \qquad (1) \qquad\qquad q_e = K_F.\,C_e^{1/nF} \qquad (2)$$

$$q_e = \frac{q_m.(K_s.C_e)^{1/n_s}}{1+(K_s.C_e)^{1/n_s}} \qquad (3) \qquad\qquad q_e = \frac{K_{RP}.C_e}{1+(a_{RP}.{C_e}^{g})} \qquad (4)$$

where q_e (mg g^{-1}) and C_e (mg L^{-1}) represent MPs adsorption capacity per unit of adsorbent and the adsorbate concentration, respectively, both at equilibrium [47].

2.5. Adsorption experiments with wastewater

Wastewater (WW) samples were collected from the secondary treatment tanks of an UWWTP located in northern Portugal. The characterization of this WW has already been reported in previous studies of our group [48, 49]. The WW was filtered through 1.2 μm glass-fiber filters (47 mm GF/C, Whatman™, Maidstone, United Kingdom) to remove suspended solids and then frozen until usage. WW samples were spiked with a stock solution containing the 20 MPs (ethanolic solution at 100 mg L^{-1} of each MP) to reach the desired initial concentration of 100 μg L^{-1} each: 6 antibiotics (ciprofloxacin, enrofloxacin, erythromycin, ofloxacin, tetracycline, trimethoprim), 3 beta-blockers (atenolol, metoprolol, propranolol), 5 multi-class pharmaceuticals (carbamazepine, diclofenac, furosemide, tramadol, warfarin), 4 herbicides (alachlor, atrazine, isoproturon, simazine), and 2 insecticides (thiacloprid, thiamethoxam). The adsorption kinetics tests were performed in amber glass flasks filled with 50 mL of spiked WW and 0.25 g L^{-1} of $ASBCM_{800}$, which were kept under stirring at room temperature for 90 min.

2.6. Analytical methods

All samples were filtered through 0.22 μm polytetrafluoroethylene (PTFE) syringe filters prior to analysis. For adsorption kinetics and equilibrium experiments using ultrapure water spiked with the 2 compounds selected as model system of organic MPs (i.e., metoprolol and diclofenac), ultra-high-performance liquid chromatography (UHPLC) was performed with a Shimadzu Corporation device (Nexera, Tokyo, Japan) furnished with an autosampler (SIL-30AC), a degasser (DGU-20A5), a system controller (CBM-20 A Lite), a column oven (CTO-20AC), a pump (LC-30AD), and a fluorescence detector (FD; RF-20AXS). A Kinetex™ 1.7 μm XB-C18 100 Å column (100 × 2.1 mm i.d.) (Phenomenex, Inc., California, USA) was used under an oven temperature set at 40 °C. The mobile phase consisted of 0.1% formic acid aqueous solution and acetonitrile (ACN), under gradient mode (15% ACN during the first 2 min; 15% to 95% ACN during 8 min; after which the initial conditions of 15% ACN were regained and kept during 7 min) at 0.20 mL min^{-1}. The volume of injection was 0.5 and 3 μL depending on initial concentration of the contaminants and the autosampler temperature was kept at 15 °C. The FD excitation and emission wavelengths were 230/290 nm for metoprolol and 285/360 nm for diclofenac.

For the analysis of WW spiked with the 20 MPs, a Shimadzu Corporation (Japan) UHPLC with tandem mass spectrometry (UHPLC-MS/MS) was used, consisting of an UHPLC equipment similar to that described above, but in this case coupled to a triple quadrupole mass spectrometer (Ultra Fast Mass Spectrometry series LCMS-8040) with an ESI source operating in both positive and negative ionization modes. The same Kinetex™ 1.7 μm XB-C18 100 Å column was employed. The same mobile phase was used, under gradient mode, with the temperature of the column oven set at 35 °C. The volume of injection was 10 μL. The determination of the target MPs was performed by selected reaction monitoring (SRM), using the most abundant fragment ion for quantification and the second most abundant to confirm the identity of each MP. The capillary voltage, drying gas and nebulizing gas flows, desolvation, and source temperatures were 4.5 kV, 15 dm^3 min^{-1}, 3.0 dm^3 min^{-1}, 400 °C, and 250 °C, respectively. Argon at 230 kPa was used as collision induced dissociation (CID) gas.

3. Results and discussion

3.1. Materials characterization

The spirulina extract used as carbon feedstock was first characterized by the TGA analysis (Figure S1a and S1b). This preliminary characterization, performed before the synthesis of the spirulina-based carbon materials (SBCM), allowed to properly select the temperature range employed in the annealing of this biomass (and activation of the resulting carbon materials). As observed, the weigh-loss during TGA performed under the inert atmosphere of N_2 goes through a maximum at ca. 350 ºC (Figure S1a), which can be ascribed to the decomposition of organic polymers such as hemicellulose (usually occurring at 200 – 320 ºC), cellulose (300 – 400 ºC) and lignin (150 – 900 ºC) [50-53]. Afterwards, as the temperature increases above ca. 550-600 ºC, the weight-loss becomes less pronounced until all the volatile content (71.6 wt.%) is decomposed at 900 ºC. On the other hand, when TGA is performed under oxidative atmosphere, the weight-loss goes through a second maximum at ca. 650-750 ºC (Figure S1b). This weight-loss can be ascribed to the carbon phase, which is resistant to high temperatures (Figure S1a) but not to thermal oxidation (Figure S1b). Having these results in mind, the pre-carbonization temperature was set at 600 ºC. This temperature allows most of the volatile content to be thermally decomposed (Figure S1a) leaving behind mostly carbon and the inorganic constituents of spirulina described in Section 2.1, which is expected to increase the effectiveness of the KOH activation step [54]. Accordingly, the carbonization/activation temperature was set at 800 ºC, i.e., to ensure that all the carbon precursors are carbonized.

The textural properties of the spirulina-based carbon materials ($SBCM_{600}$, and $SBCM_{800}$, and $ASBCM_{800}$) were characterized from N_2 adsorption–desorption isotherms (Figure 1). The corresponding results are given in Table 1. Both $SBCM_{600}$, and $SBCM_{800}$ are essentially non-porous materials, with no microporosity and negligible mesoporosity, as indicated by the absence and negligible N_2 adsorption at low and high relative pressures, respectively (Figure 1). These observations are confirmed by the values of S_{BET} obtained for these non-activated materials, which are within the experimental error of the determination (ca. 5 $m^2\ g^{-1}$; Table 1). On the contrary, $ASBCM_{800}$ has a well-developed porosity, arising mainly from micropores (Figure 1). As consequence, the S_{BET} of this activated material ($ASBCM_{800}$) is surprisingly high (2211 $m^2\ g^{-1}$; Table 1), even compared to the values previously reported for spirulina-derived biochars thermally treated at 350, 550, or 750 °C (0.31, 1.55 and 2.63 $m^2\ g^{-1}$, respectively) [7]. Moreover, the V_{Total} of $ASBCM_{800}$ accounts to 0.990 $cm^3\ g^{-1}$ (mostly from micropores, having a ratio V_{micro}/V_{Total} of 0.86). The superior surface area and porosity of $ASBCM_{800}$ confirms the effectiveness of the approach taken, namely pre-carbonization of spirulina followed by chemical activation with KOH at 800 ºC. In the case of $ASBCM_{800}$, microporous account for more than 85% of all porosity. The pH_{PZC} of $ASBCM_{800}$ was ca. 8.4, a similar value to that revealed by Choi *et al.*, [7] of 8.3 for a spirulina-derived biochar thermally treated at 750 ºC.

Table 1. Textural properties of the spirulina-based carbon materials: specific surface area (S_{BET}), non-microporous specific surface area (S_{meso}), micropore volume (V_{micro}), and total pore volume (V_{total}).

Material	S_{BET} (m^2 g^{-1})	S_{meso} (m^2 g^{-1})	V_{micro} (cm^3 g^{-1})	V_{total} (cm^3 g^{-1})
$SBCM_{600}$	4*	4*	0.000	0.005
$SBCM_{800}$	5*	5*	0.000	0.009
$ASBCM_{800}$	2211	130	0.849	0.990

*within the experimental error of the determination (ca. 5 m^2 g^{-1})

Since porosity is a crucial feature for adsorption applications, the non-activated materials ($SBCM_{600}$ and $SBCM_{800}$) were not considered in the subsequent studies. $ASBCM_{800}$ was further characterized, namely by FTIR-ATR, TGA, SEM-EDS, TEM and XPS analyses.

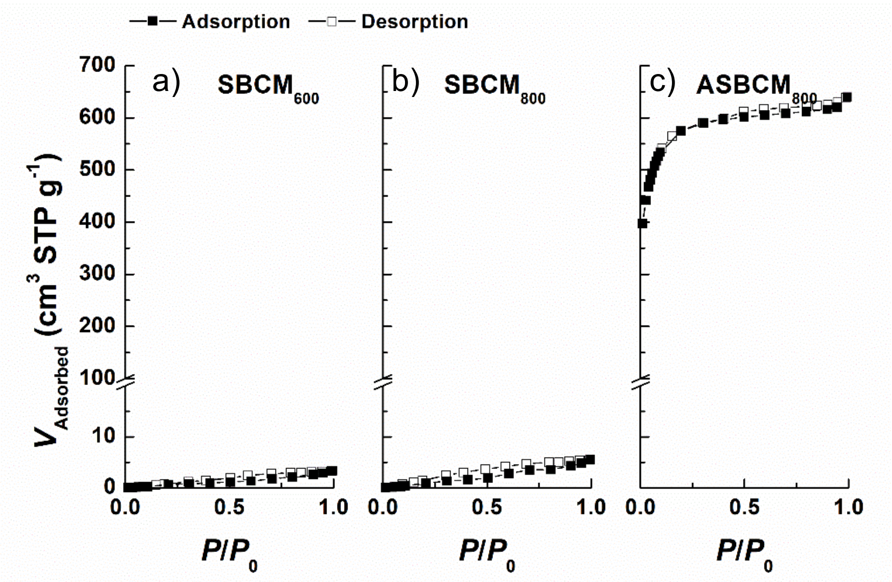

Figure 1. N_2 adsorption–desorption isotherms of the tested materials: a) $SBCM_{600}$, b) $SBCM_{800}$, and c) $ASBCM_{800}$.

Several peaks are observed in the FTIR-ATR spectrum of spirulina (Figure 2), namely at ca. 3350 cm^{-1} (corresponding to -OH band), ca. 2930 cm^{-1} (C-H stretching), ca. 1640 cm^{-1} (aromatic conjugated C=O and C=C bonds), ca. 1520 cm^{-1} (N-H bending and C-N stretching), ca. 1430 cm^{-1} (C-H bending), ca. 1375 cm^{-1}

(C=O carboxylate stretching), ca. 1270 cm^{-1} (C-OH phenolics), C-O single bonds (1150 cm^{-1}), ca. 1050 cm^{-1} (C-O stretching), and ca. 875 cm^{-1} (CO_3^{2-}), which agree with the findings previously reported in other studies dealing with biomass [7, 55]. These strong and easily identifiable peaks are not observed in the FTIR-ATR spectrum of $ASBCM_{800}$ (Figure 2), thus confirming the loss of functional groups during the thermal treatment. These results are in accordance with those previously observed by TGA, in which the decomposition of organic polymers of spirulina (such as hemicellulose, cellulose, and lignin) was found to occur mainly at ca. 350 ºC (Figure S1a), and agree also with previous reports [7, 55]. In turn, the $ASBCM_{800}$ sample reveals a high resistance to temperature and a low volatile content (10.5 wt.%; Figure S1c), as well as an ash content of 19.6 wt.% (Figure S1c), which can be ascribed to the inorganic constituents of spirulina described in Section 2.1, some detected by EDS (mostly Fe, Ca, Mg, K, and Si; Figure S2b-e). Moreover, the carbon content of $ASBCM_{800}$ can be estimated as 69.9 wt.%, i.e., the fraction not corresponding to volatiles (10.5 wt.%) or ashes (19.6 wt.%).

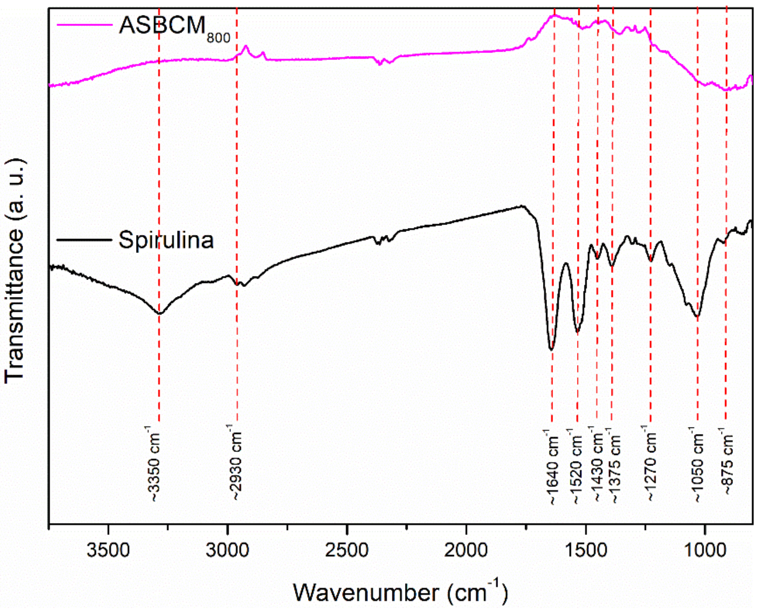

Figure 2. FTIR-ATR spectra of commercial spirulina extract and $ASBCM_{800}$.

The SEM images of $ASBCM_{800}$ (Figure 3a and b) reveal particles with different sizes and smooth surfaces with some breaks. Some brilliant points (Figure 3a and b, and Figures S2a and S2c (Z3)), and fibers or fiber bundles (Figure 3b, Figures S2a, S2d (Z4), and S2e (Z5)) are observed using the BSED, which indicate the occurrence of Ca and Fe, respectively. The SEM images of the raw spirulina sample with a thin film coating of Au/Pd (Figure 3c and d, and Figures S3a and d) show dehydrated microalgae cells with different sizes. Again, some brilliant points were observed, particularly in Figure S3a (Z1 EDS spectrum in Figure S3b, indicating the occurrence of P and K) and Figure S3d (Z6 EDS spectrum in Figure S3e, demonstrating the presence of P, K, Si, and Al). Other elements were found in both samples, such as C, O, K, Si, and Mg. However, Fe was only found in ASBCM$_{800}$; while N, P, Na, S, Al, and Cl were only observed in the EDS of spirulina [7, 38].

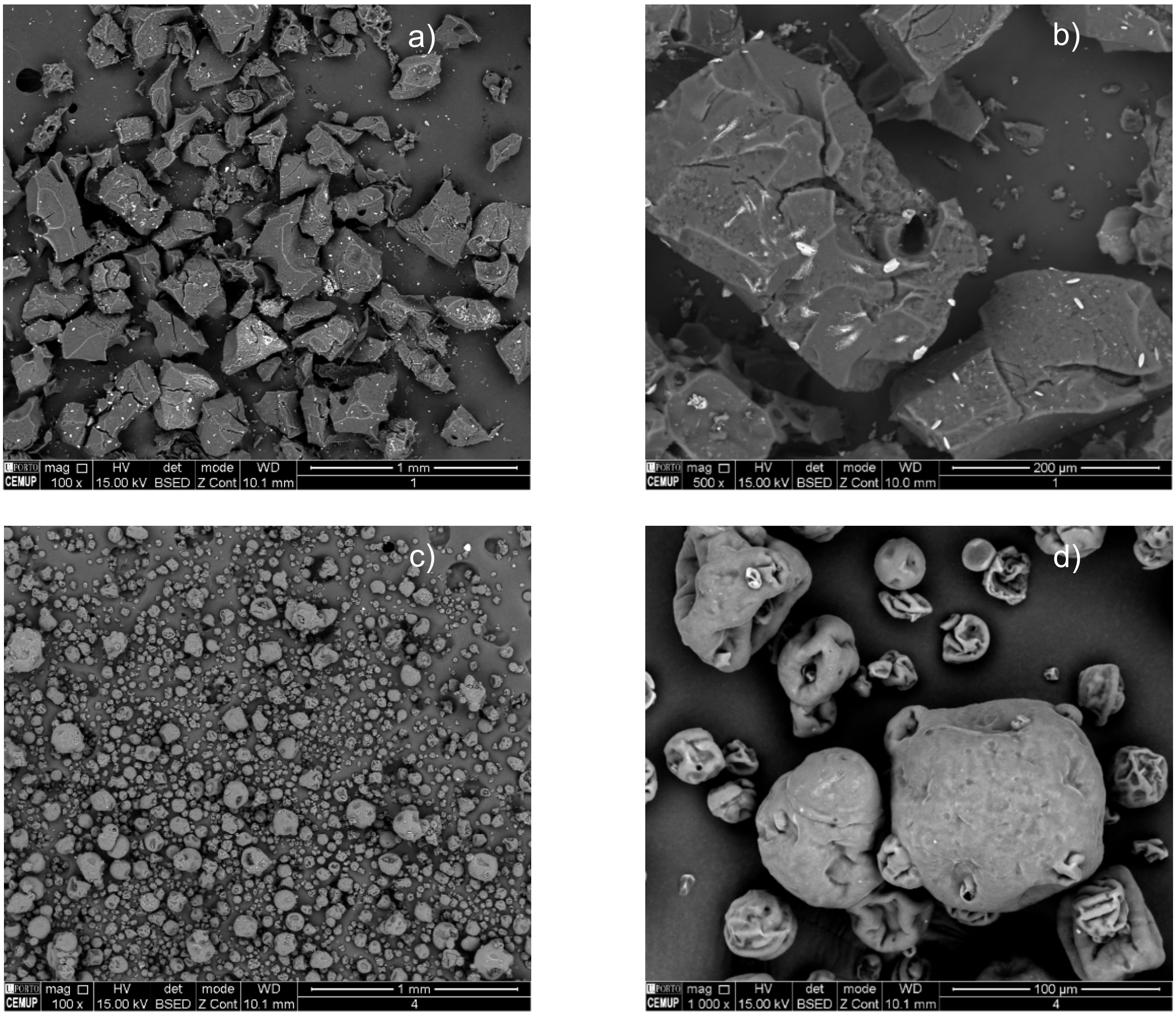

Figure 3. SEM images collected in BSED mode of the ASBCM800 biosorbent (a and b) and commercially available spirulina extract from Celeiro© (coated with an Au/Pd thin film) (c and d) with magnifications of 100 x (a and c) and 500 x (b and d).

The TEM image of ASBCM$_{800}$ (Figure 4) revealed the presence of nano-spherical particles, originated from the algae-constituents, depicting a heterogeneous surface of ASBCM$_{800}$. However, these algae species are well dispersed on the activated carbon surface and the average diameters of the particles are in the range of 50-

170 nm. Additionally, the presence of inorganic (metalic/non-metalic) species on activated carbon surface tend to agglomerate with KOH activation; such morphology may be dispersed in an amorphous carbon matrix (as shown in Figure 4b) [56].

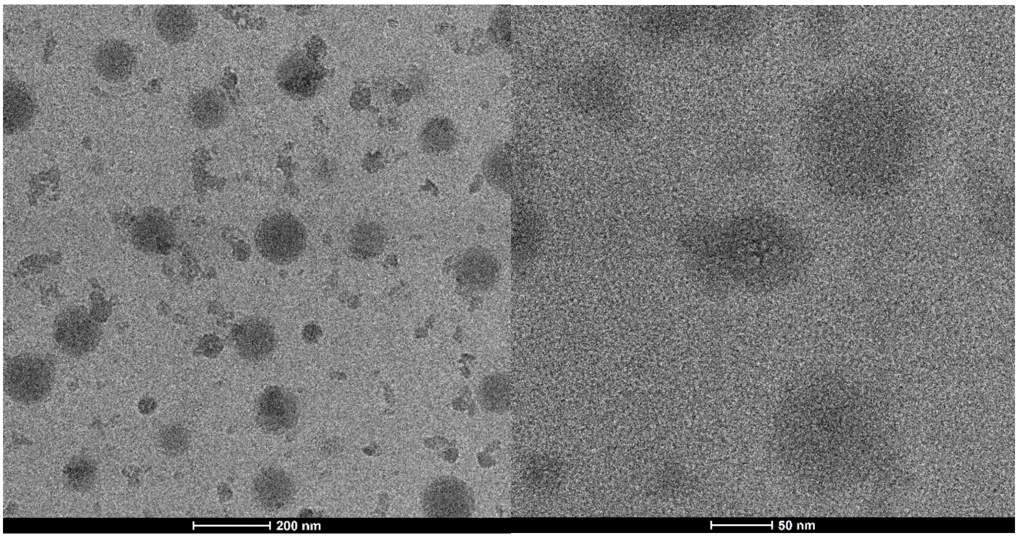

Figure 4. TEM images of ASBCM$_{800}$.

The XPS spectrum of ASBCM$_{800}$ is presented in Figure 5, where the survey spectrum shows the photoelectron lines of the main elements. The chemical composition provided by the XPS analysis is complementary to the EDS analysis, confirming the presence of the most dominant elements in the following order: C (41.93 At %), O (23.48 At %), K (14.29 At %), Mg (14.15 At %), Si (3.90 At %) and Ca (2.25 At %). The percentage of carbon present in the ASBCM$_{800}$ sample was significantly higher compared to the other elements, which confirmed that the adsorbent was carbonaceous and had developed active micropore sites available to be occupied with the organic species (in accordance with data shown in Table 1). Therefore, the comprehensive textural and morphological characterization results suggest that ASBCM$_{800}$ possesses prosperous adsorptive properties.

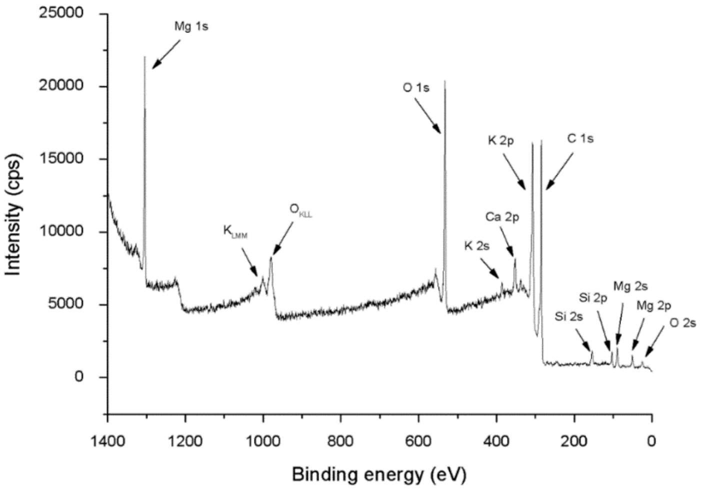

Figure 5. XPS survey spectrum of $ASBCM_{800}$.

3.2. Adsorption kinetic experiments with metoprolol and diclofenac

The adsorption kinetics of metoprolol and diclofenac onto $ASBCM_{800}$ were studied separately, considering 1 mg L^{-1} solutions of each compound used as model systems (Figure 6). These compounds were selected due to their environmental relevance as contaminants of emerging concern (CECs): metoprolol is an unregulated compound of emerging concern [1, 57] and diclofenac was temporarily included in the watch list of substances referred in Article 8b of Directive 2008/105/EC set out in the Annex of the European Decision 2015/495 [58]. As observed, $ASBCM_{800}$ possesses a high adsorption affinity towards both metoprolol and diclofenac, as indicated by the complete removal of the target analytes in ca. 20 min (Figure 6). This performance can be explained by the well-developed surface area and porosity of the $ASBCM_{800}$ (section 3.1).

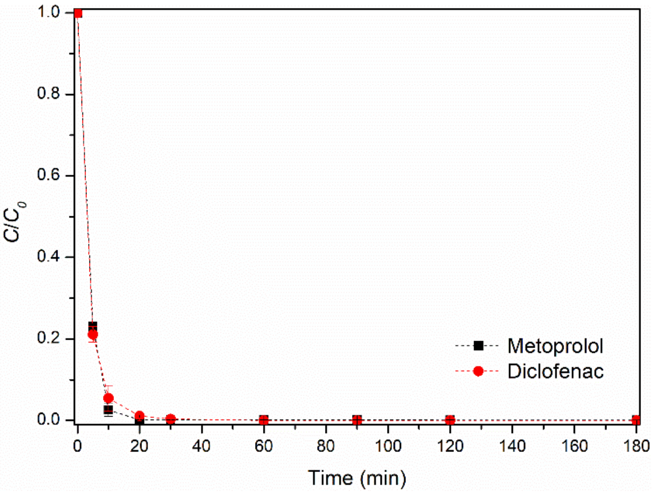

Figure 6. Normalized concentration of metoprolol and diclofenac over time in adsorption experiments performed with 50 mL of individual solutions containing 1 mg L^{-1} of either metoprolol or diclofenac (under stirring), 0.25 g L^{-1} of $ASBCM_{800}$, natural pH, and $T = 25$ °C.

3.3. Equilibrium adsorption experiments with metoprolol and diclofenac

Individual adsorption equilibrium isotherms were obtained with 0.25 g L^{-1} of $ASBCM_{800}$ and metoprolol or diclofenac solutions with different initial concentrations (Figure 7a and b, respectively).

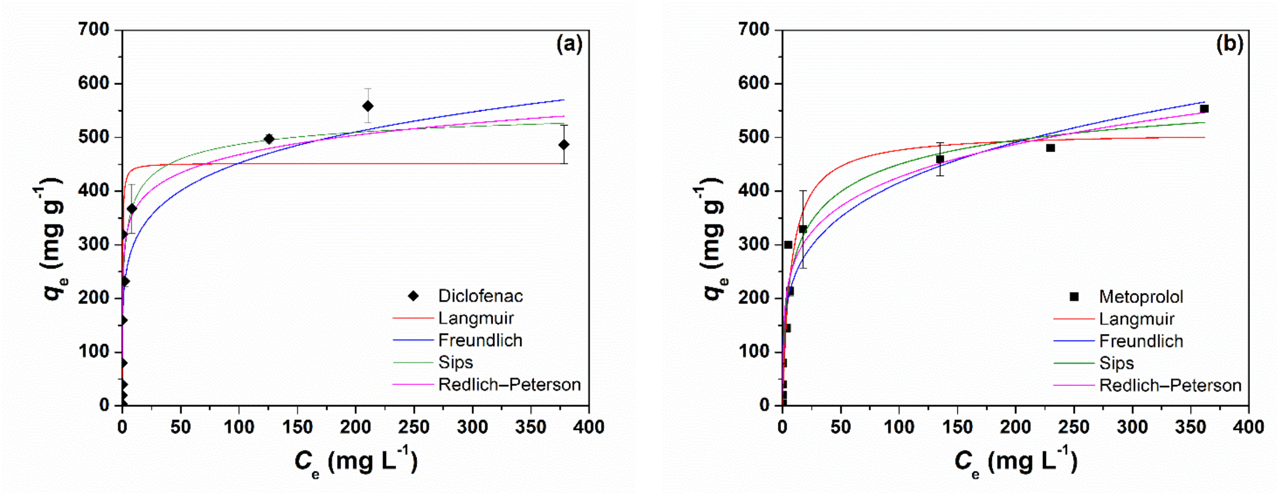

Figure 7. Adsorption isotherms for diclofenac (a) and metoprolol (b) onto $ASBCM_{800}$. Conditions: 10 mL of individual solutions containing 1 mg L^{-1} of either metoprolol or diclofenac and 0.25 g L^{-1} of $ASBCM_{800}$, natural pH, $T = 25$ °C, stirring for 5 days.

Langmuir isotherm model assumes a homogenous adsorbing surface, where all sites experience a monolayer-type adsorption with insignificant interactions between the MP molecules [6, 59]. In this model, q_{sat} refers to the maximum adsorption capacity and b is associated to adsorption intensity [47]. On the other hand, the Freundlich model describes heterogeneous systems and does not suggest a limited uptake capacity of the adsorbent, therefore it may be applied only in the low-intermediate adsorbate concentration ranges [60]. In this isotherm, K_F and n_F parameters define the adsorption capacity (the Freundlich constant K_F) and intensity (n_F), respectively [47]. From the combination of the Langmuir and Freundlich isotherm models, it results the Sips model, which is likely to better describe heterogeneous surfaces. Depending on the adsorbate concentration, Sips model can approach the Freundlich (low concentrations) or the Langmuir (high concentrations) isotherms [60]. In the Sips model, n_s is a constant related with the adsorbent heterogeneity [47, 60], q_m correlates to the maximum adsorption capacity [47] and K_s is the Sips constant associated to adsorption intensity [47]. Another 3-parameter equation (*i.e.,* other than Sips) is Redlich–Peterson that can also be used to explain the heterogeneity of the adsorbents, with the site energy distribution function having advantages owing to the restricting conditions used [59]. The Redlich–Peterson isotherm may converge to Langmuir (when g values are equal to 1 [59]) or a Freundlich model (when the K_{RP} and a_{RP} are much greater than 1 and $g < 1$) [61]. In this model, K_{RP} and a_{RP} are the isotherm constants and g is the exponent indicating the adsorbent heterogeneity, occurring between 0 and 1 [61].

The coefficient of determination (r^2) was used to predict the best fitting to the experimental data, being the more complex 3-parameter models (Redlich-Peterson and Sips), the most suitable for diclofenac and metoprolol adsorption by $\mathrm{ASBCM_{800}}$, in comparison to the 2-parameter models (Langmuir and Freundlich), which could be an indicator of adsorbent heterogeneity. According to the results (Figure 7, Table 2), $\mathrm{ASBCM_{800}}$ can be applied as an efficient adsorbent for the 2 target MPs, diclofenac and metoprolol, thus being a desirable carbon material obtained from eco-friendly and sustainable sources (*e.g.*, lakes with microalgae), serving a double function of controlling lake eutrophication and being the precursor of value-added adsorbent materials by upcycling microalgae, such as *Spirulina* sp.

Table 2. Adsorption isotherm parameters for the adsorption of diclofenac and metoprolol onto ASBCM$_{800}$.

	Langmuir			**Freundlich**			**Sips**				**Redlich-Peterson**			
Micropollutants	q_{sat} **(mg g^{-1})**	b **(L mg^{-1})**	r^2	K_F **(L$^{1/n_F}$ mg$^{1-1/n_F}$ g^{-1})**	n_F	r^2	q_m **(mg g^{-1})**	K_S **(L^{n_S} mg$^{-n_S}$)**	n_S	r^2	K_{RP} **(L g^{-1})**	a_{RP} **(mg^{-1})**	g	r^2
Diclofenac	452.3	4.05	0.772	202.9	5.74	0.812	588.9	0.40	2.36	0.851	3421.6	11.93	0.89	0.857
Metoprolol	510.7	0.14	0.946	137.8	4.17	0.944	660.5	0.05	2.06	0.966	809.6	4.55	0.81	0.966

The parameters of the Langmuir, Freundlich, Sips, and Redlich–Peterson isotherm adsorption models were calculated using nonlinear regression with OriginPro software (Version 2019b).

3.4. Adsorption experiments with wastewater after the secondary treatment

In order to test the feasibility of $ASBCM_{800}$ to be used in real scale applications, secondary wastewater effluent samples spiked with 20 MPs belonging to 5 different classes, and including the above-mentioned target MPs (diclofenac and metoprolol) were treated with 0.25 g L^{-1} of $ASBCM_{800}$ adsorbent (Figure 8 and Figure S4). $ASBCM_{800}$ revealed a high removal performance in a very complex water matrix (i.e., wastewater), most of the MPs being adsorbed above 88% in less than 30 min (*e.g.*, ciprofloxacin, enrofloxacin, erythromycin, ofloxacin, tetracycline, trimethoprim, atenolol, metoprolol, propranolol, diclofenac, furosemide, tramadol, alachlor, atrazine, isoproturon, simazine, and thiamethoxam). From the 20 target MPs, warfarin, carbamazepine, thiacloprid were those less removed. Nevertheless, removals of more than 64% were obtained in the same period of time. *Spirulina* sp. and/or its derivatives have been applied mainly in the adsorption of dyes [6, 34-42], and metals (*e.g.*, Cr [14-19], Co [14], Pb [20-25], Zn [22, 26, 27], Fe [10], U [28], Cd [19, 23, 29, 30], Cu [18, 19, 31-33], Ni [18, 22, 23, 31], Al [31]). Thus, the evaluation of their adsorptive performance for hazardous organic MPs is scarce in the literature. Considering other organic compounds, Dotto *et al.*, [43] and Choi *et al.,* [7] tested respectively the adsorption of phenol to bionanoparticles from *Spirulina* sp. [43] and of tetracycline to *Spirulina* sp.-derived biochars [7]. To the best of our knowledge, this work reveals for the first time the successful application of spirulina-based carbon materials for the removal of several MPs from urban wastewater, showing the feasibility of using this bio-based material to remove organic contaminants from very complex matrices.

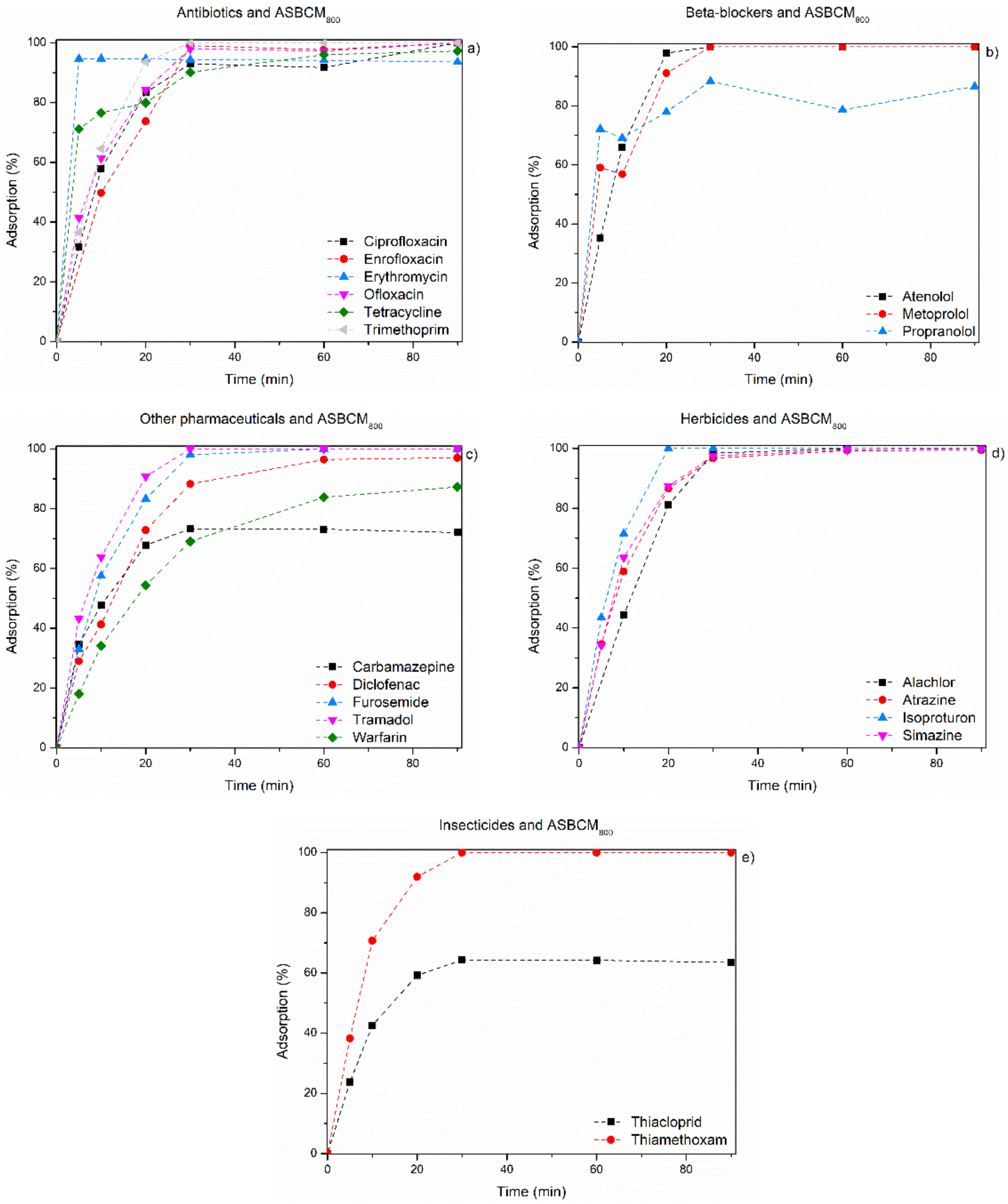

Figure 8. Adsorption of 20 MPs spiked in urban wastewater onto ASBCM$_{800}$: (a) 6 antibiotics (ciprofloxacin, enrofloxacin, erythromycin, ofloxacin, tetracycline, trimethoprim), (b) 3 beta-blockers (atenolol, metoprolol, propranolol), (c) 5 multi-class pharmaceuticals (carbamazepine, diclofenac, furosemide, tramadol, warfarin), (d) 4 herbicides (alachlor, atrazine, isoproturon, simazine), and (e) 2 insecticides (thiacloprid, thiamethoxam). Conditions: 50 mL of spiked wastewater containing 100 µg L^{-1} of each MP and 0.25 g L^{-1} of ASBCM$_{800}$, natural pH, T = 25 °C, stirring for 90 min.

4. Conclusions

This study consolidates a simple material design (2-step approach) and a comprehensive characterization of a spirulina-based carbon material towards its potential up-scaling in engineering applications. The potential application of a microalgae-based carbon material with advanced porosity as an effective way to remove MPs from heterogeneous and complex matrices, was demonstrated. The synthesized material was proven as adequate for the treatment of urban wastewaters spiked with 20 trace MPs having different origin and classification. The activated spirulina-based carbon material yielded an overall removal of 75% for the 20 MPs, from which 17 were adsorbed by more than 88%. The significance of using this biologically originated carbon material is reflected by the resource recovery of a natural material, the contribution to control algal blooms and to mitigate eutrophication.

Conflicts of interest

The authors declare no known competing financial interests or personal relationships affecting the research or conclusions of the work published.

Acknowledgments

This work was financially supported by Project POCI-01-0145-FEDER-030521 funded by ERDF funds through COMPETE2020—POCI and by National Funds (PIDDAC) through FCT/MCTES. We would also like to thank the scientific collaboration under LA/P/0045/2020 (ALiCE), UIDB/50020/2020 and UIDP/50020/2020 (LSRE-LCM), funded by national funds through FCT/MCTES (PIDDAC) and project Healthy Water - Identification, Elimination, Social Awareness and Education of Water Chemical and Biological Micropollutants with Health and Environmental Implications, with reference NORTE-01-0145-FEDER-000069, supported by Norte Portugal Regional Operational Programme (NORTE 2020), under the PORTUGAL 2020 Partnership Agreement through the European Regional Development Fund (ERDF).

ARLR acknowledges FCT funding under DL57/2016 Transitory Norm Programme. MBĐ acknowledges to the Ministry of Education, Science and Technological Development of the Republic of Serbia (Contract

No. 451-03-9/2021-14/200135). SGR acknowledges Universidad Politécnica de Madrid (UPM) for the financial support given through the predoctoral contract granted within the "Programa Propio". JRC acknowledges Comunidad de Madrid for funding the research project IN_REUSE (APOYO-JOVENES-X5PKL6-88-KZ46KU) within the framework of the multi-year agreement with the Universidad Politécnica de Madrid, and also by the Pluriannual Agreement with the Polytechnic University of Madrid in the line of action Programme of Excellence for University Teaching Staff". Technical assistance with SEM analysis is gratefully acknowledged to CEMUP team.

Disclaimer

The research and conclusions thereof of this work are declared to be under the responsibility of the authors themselves. No third party is to be held responsible.

References

[1] J.C.G. Sousa, A.R. Ribeiro, M.O. Barbosa, M.F.R. Pereira, A.M.T. Silva, A review on environmental monitoring of water organic pollutants identified by EU guidelines, Journal of Hazardous Materials, 344 (2018) 146-162.

[2] M.O. Barbosa, N.F.F. Moreira, A.R. Ribeiro, M.F.R. Pereira, A.M.T. Silva, Occurrence and removal of organic micropollutants: An overview of the watch list of EU Decision 2015/495, Water research, 94 (2016) 257-279.

[3] A.R. Ribeiro, O.C. Nunes, M.F. Pereira, A.M. Silva, An overview on the advanced oxidation processes applied for the treatment of water pollutants defined in the recently launched Directive 2013/39/EU, Environment international, 75 (2015) 33-51.

[4] G. Crini, E. Lichtfouse, Advantages and disadvantages of techniques used for wastewater treatment, Environmental Chemistry Letters, 17 (2019) 145-155.

[5] G. Crini, E. Lichtfouse, L.D. Wilson, N. Morin-Crini, Conventional and non-conventional adsorbents for wastewater treatment, Environmental Chemistry Letters, 17 (2019) 195-213.

[6] P. Nautiyal, K.A. Subramanian, M.G. Dastidar, Adsorptive removal of dye using biochar derived from residual algae after in-situ transesterification: Alternate use of waste of biodiesel industry, Journal of Environmental Management, 182 (2016) 187-197.

[7] Y.K. Choi, T.R. Choi, R. Gurav, S.K. Bhatia, Y.L. Park, H.J. Kim, E. Kan, Y.H. Yang, Adsorption behavior of tetracycline onto Spirulina sp. (microalgae)-derived biochars produced at different temperatures, Sci Total Environ, 710 (2020) 136282.

[8] H.C. Lee, M. Lee, W. Den, Spirulina maxima for phenol removal: Study on its tolerance, biodegradability and phenol-carbon assimilability, Water, Air, and Soil Pollution, 226 (2015).

[9] X.J. Lee, H.C. Ong, J. Ooi, K.L. Yu, T.C. Tham, W.-H. Chen, Y.S. Ok, Engineered macroalgal and microalgal adsorbents: Synthesis routes and adsorptive performance on hazardous water contaminants, Journal of Hazardous Materials, 423 (2022) 126921.

[10] M.A. Fawzy, M. Gomaa, Use of algal biorefinery waste and waste office paper in the development of xerogels: A low cost and eco-friendly biosorbent for the effective removal of congo red and Fe (II) from aqueous solutions, Journal of Environmental Management, 262 (2020).

[11] M.A. Fawzy, Fatty Acid Characterization and Biodiesel Production by the Marine Microalga Asteromonas gracilis: Statistical Optimization of Medium for Biomass and Lipid Enhancement, Marine Biotechnology, 19 (2017) 219-231.

[12] J. Masojídek, G. Torzillo, Mass Cultivation of Freshwater Microalgae☆, in: Reference Module in Earth Systems and Environmental Sciences, Elsevier, 2014.

[13] E. Koru, Earth Food Spirulina (*Arthrospira*): Production and Quality Standarts, in: Food Additive, 2012.

[14] K. Nithya, A. Sathish, K. Pradeep, S. Kiran Baalaji, Algal biomass waste residues of Spirulina platensis for chromium adsorption and modeling studies, Journal of Environmental Chemical Engineering, 7 (2019) 103273.

[15] E. Gunasundari, P.S. Kumar, Higher adsorption capacity of Spirulina platensis alga for Cr(VI) ions removal: Parameter optimisation, equilibrium, kinetic and thermodynamic predictions, IET Nanobiotechnology, 11 (2017) 317-328.

[16] L.M. Colla, C. Dal'Magro, A. De Rossi, A. Thomé, C.O. Reinehr, T.E. Bertolin, J.A.V. Costa, Potential of Live Spirulina platensis on Biosorption of Hexavalent Chromium and Its Conversion to Trivalent Chromium, International Journal of Phytoremediation, 17 (2015) 861-868.

[17] A. Lodi, D. Soletto, C. Solisio, A. Converti, Chromium(III) removal by *Spirulina platensis* biomass, Chemical Engineering Journal, 136 (2008) 151-155.

[18] H. Doshi, A. Ray, I.L. Kothari, Bioremediation potential of live and dead Spirulina: Spectroscopic, kinetics and SEM studies, Biotechnology and Bioengineering, 96 (2007) 1051-1063.

[19] K. Chojnacka, A. Chojnacki, H. Górecka, Biosorption of Cr^{3+}, Cd^{2+} and Cu^{2+} ions by blue-green algae *Spirulina* sp.: Kinetics, equilibrium and the mechanism of the process, Chemosphere, 59 (2005) 75-84.

[20] X. Sun, H. Huang, D. Zhao, J. Lin, P. Gao, L. Yao, Adsorption of Pb2+ onto freeze-dried microalgae and environmental risk assessment, Journal of Environmental Management, 265 (2020) 110472.

[21] A.A. Al-Homaidan, A.F. Al-Abbad, A.A. Al-Hazzani, A.A. Al-Ghanayem, J.A. Alabdullatif, Lead removal by Spirulina platensis biomass, International Journal of Phytoremediation, 18 (2016) 184-189.

[22] M.S. Rodrigues, L.S. Ferreira, J.C.M.D. Carvalho, A. Lodi, E. Finocchio, A. Converti, Metal biosorption onto dry biomass of Arthrospira (Spirulina) platensis and Chlorella vulgaris: Multi-metal systems, Journal of Hazardous Materials, 217-218 (2012) 246-255.

[23] A. Şeker, T. Shahwan, A.E. Eroğlu, S. Yilmaz, Z. Demirel, M.C. Dalay, Equilibrium, thermodynamic and kinetic studies for the biosorption of aqueous lead(II), cadmium(II) and nickel(II) ions on *Spirulina platensis*, Journal of Hazardous Materials, 154 (2008) 973-980.

[24] H. Chen, S.S. Pan, Bioremediation potential of spirulina: Toxicity and biosorption studies of lead, Journal of Zhejiang University: Science, 6 B (2005) 171-174.

[25] R. Gong, Y. Ding, H. Liu, Q. Chen, Z. Liu, Lead biosorption and desorption by intact and pretreated *spirulina maxima* biomass, Chemosphere, 58 (2005) 125-130.

[26] I. Zinicovscaia, N. Yushin, M. Shvetsova, M. Frontasyeva, Zinc removal from model solution and wastewater by Arthrospira (Spirulina) Platensis biomass, International Journal of Phytoremediation, 20 (2018) 901-908.

[27] A. Kőnig-Péter, C. Csudai, A. Felinger, F. Kilár, T. Pernyeszi, Potential of various biosorbents for Zn(II) removal, Water, Air, and Soil Pollution, 225 (2014).

[28] G. Bayramoglu, A. Akbulut, M.Y. Arica, Study of polyethyleneimine- and amidoxime-functionalized hybrid biomass of Spirulina (Arthrospira) platensis for adsorption of uranium (VI) ion, Environmental Science and Pollution Research, 22 (2015) 17998-18010.

[29] C. Solisio, A. Lodi, D. Soletto, A. Converti, Cadmium biosorption on *Spirulina platensis* biomass, Bioresource Technology, 99 (2008) 5933-5937.

[30] H.Y. Wang, F. Yang, W.J. Zheng, Y. Bai, Growth and Cd uptake of Spirulina in water body containing $CdCl_2$, Chinese Journal of Applied Ecology, 18 (2007) 1917-1920.

[31] F. Almomani, R.R. Bhosale, Bio-sorption of toxic metals from industrial wastewater by algae strains Spirulina platensis and Chlorella vulgaris: Application of isotherm, kinetic models and process optimization, Science of The Total Environment, 755 (2021) 142654.

[32] A. Çelekli, M. Yavuzatmaca, H. Bozkurt, An eco-friendly process: Predictive modelling of copper adsorption from aqueous solution on *Spirulina platensis*, Journal of Hazardous Materials, 173 (2010) 123-129.

[33] C. Solisio, A. Lodi, P. Torre, A. Converti, M. Del Borghi, Copper removal by dry and re-hydrated biomass of *Spirulina platensis*, Bioresource Technology, 97 (2006) 1756-1760.

[34] N.F. Cardoso, E.C. Lima, B. Royer, M.V. Bach, G.L. Dotto, L.A.A. Pinto, T. Calvete, Comparison of Spirulina platensis microalgae and commercial activated carbon as adsorbents for the removal of Reactive Red 120 dye from aqueous effluents, Journal of Hazardous Materials, 241-242 (2012) 146-153.

[35] M.H. Marzbali, A.A. Mir, M. Pazoki, R. Pourjamshidian, M. Tabeshnia, Removal of direct yellow 12 from aqueous solution by adsorption onto spirulina algae as a high-efficiency adsorbent, Journal of Environmental Chemical Engineering, 5 (2017) 1946-1956.

[36] Z. Yang, J. Hou, L. Miao, J. Wu, Comparison of adsorption behavior studies of methylene blue by microalga residue and its biochars produced at different pyrolytic temperatures, Environmental Science and Pollution Research, 28 (2021) 14028-14040.

[37] G.L. Dotto, L.A.A. Pinto, Analysis of mass transfer kinetics in the biosorption of synthetic dyes onto Spirulina platensis nanoparticles, Biochemical Engineering Journal, 68 (2012) 85-90.

[38] G.L. Dotto, E.C. Lima, L.A.A. Pinto, Biosorption of food dyes onto Spirulina platensis nanoparticles: Equilibrium isotherm and thermodynamic analysis, Bioresource Technology, 103 (2012) 123-130.

[39] G.L. Dotto, V.M. Esquerdo, M.L.G. Vieira, L.A.A. Pinto, Optimization and kinetic analysis of food dyes biosorption by Spirulina platensis, Colloids and Surfaces B: Biointerfaces, 91 (2012) 234-241.

[40] G.L. Dotto, T.R.S. Cadaval, L.A.A. Pinto, Use of Spirulina platensis micro and nanoparticles for the removal synthetic dyes from aqueous solutions by biosorption, Process Biochemistry, 47 (2012) 1335-1343.

[41] F. Robledo-Padilla, O. Aquines, A. Silva-Núñez, G.S. Alemán-Nava, C. Castillo-Zacarías, R.A. Ramirez-Mendoza, R. Zavala-Yoe, H.M.N. Iqbal, R. Parra-Saldívar, Evaluation and Predictive Modeling of Removal Condition for Bioadsorption of Indigo Blue Dye by Spirulina platensis, Microorganisms, 8 (2020) 82.

[42] X. Tan, S. Zhu, P.L. Show, H. Qi, S.H. Ho, Sorption of ionized dyes on high-salinity microalgal residue derived biochar: Electron acceptor-donor and metal-organic bridging mechanisms, Journal of Hazardous Materials, 393 (2020).

[43] G.L. Dotto, J.O. Gonçalves, T.R.S. Cadaval, L.A.A. Pinto, Biosorption of phenol onto bionanoparticles from Spirulina sp. LEB 18, Journal of Colloid and Interface Science, 407 (2013) 450-456.

[44] R.S. Ribeiro, Z. Frontistis, D. Mantzavinos, D. Venieri, M. Antonopoulou, I. Konstantinou, A.M.T. Silva, J.L. Faria, H.T. Gomes, Magnetic carbon xerogels for the catalytic wet peroxide oxidation of sulfamethoxazole in environmentally relevant water matrices, Applied Catalysis B: Environmental, 199 (2016) 170-186.

[45] L.M. Pastrana-Martinez, S. Morales-Torres, J.L. Figueiredo, J.L. Faria, A.M.T. Silva, Graphene oxide based ultrafiltration membranes for photocatalytic degradation of organic pollutants in salty water, Water research, 77 (2015) 179-190.

[46] M. Pedrosa, E.S. Da Silva, L.M. Pastrana-Martínez, G. Drazic, P. Falaras, J.L. Faria, J.L. Figueiredo, A.M.T. Silva, Hummers' and Brodie's graphene oxides as photocatalysts for phenol degradation, Journal of Colloid and Interface Science, 567 (2020) 243-255.

[47] S. Álvarez, R.S. Ribeiro, H.T. Gomes, J.L. Sotelo, J. García, Synthesis of carbon xerogels and their application in adsorption studies of caffeine and diclofenac as emerging contaminants, Chemical Engineering Research and Design, 95 (2015) 229-238.

[48] S. Guerra-Rodríguez, A.R.L. Ribeiro, R.S. Ribeiro, E. Rodríguez, A.M.T. Silva, J. Rodríguez-Chueca, UV-A activation of peroxymonosulfate for the removal of micropollutants from secondary treated wastewater, Science of The Total Environment, 770 (2021) 145299.

[49] C.A.L. Graça, S. Ribeirinho-Soares, J. Abreu-Silva, I.I. Ramos, A.R. Ribeiro, S.M. Castro-Silva, M.A. Segundo, C.M. Manaia, O.C. Nunes, A.M.T. Silva, A Pilot Study Combining Ultrafiltration with Ozonation for

the Treatment of Secondary Urban Wastewater: Organic Micropollutants, Microbial Load and Biological Effects, Water, 12 (2020) 3458.

[50] C.L. Waters, R.R. Janupala, R.G. Mallinson, L.L. Lobban, Staged thermal fractionation for segregation of lignin and cellulose pyrolysis products: An experimental study of residence time and temperature effects, Journal of Analytical and Applied Pyrolysis, 126 (2017) 380-389.

[51] H. Yang, R. Yan, H. Chen, D.H. Lee, C. Zheng, Characteristics of hemicellulose, cellulose and lignin pyrolysis, Fuel, 86 (2007) 1781-1788.

[52] D. Lv, M. Xu, X. Liu, Z. Zhan, Z. Li, H. Yao, Effect of cellulose, lignin, alkali and alkaline earth metallic species on biomass pyrolysis and gasification, Fuel Processing Technology, 91 (2010) 903-909.

[53] G. Várhegyi, M.J. Antal, E. Jakab, P. Szabó, Kinetic modeling of biomass pyrolysis, Journal of Analytical and Applied Pyrolysis, 42 (1997) 73-87.

[54] L. Chunlan, X. Shaoping, G. Yixiong, L. Shuqin, L. Changhou, Effect of pre-carbonization of petroleum cokes on chemical activation process with KOH, Carbon, 43 (2005) 2295-2301.

[55] R.R. Domingues, P.F. Trugilho, C.A. Silva, I.C.N.A.d. Melo, L.C.A. Melo, Z.M. Magriotis, M.A. Sánchez-Monedero, Properties of biochar derived from wood and high-nutrient biomasses with the aim of agronomic and environmental benefits, PLOS ONE, 12 (2017) e0176884.

[56] C. Saka, Phosphorus and oxygen doped carbon-based on Spirulina microalgae as efficient metal-free catalysts to obtain H_2 from methanolysis of $NaBH_4$, International Journal of Hydrogen Energy, 46 (2021) 3753-3762.

[57] M.O. Barbosa, A.R. Ribeiro, M.F.R. Pereira, A.M.T. Silva, Eco-friendly LC–MS/MS method for analysis of multi-class micropollutants in tap, fountain, and well water from northern Portugal, Analytical and Bioanalytical Chemistry, 408 (2016) 8355-8367.

[58] Decision 2015/495/EU of 20 March 2015 establishing a watch list of substances for Union-wide monitoring in the field of water policy pursuant to Directive 2008/105/EC of the European Parliament and of the Council, in: T.E.P.a.t.C.o.t.E. Union (Ed.) Official Journal of the European Union, 2015, pp. 40-42.

[59] M. Belhachemi, F. Addoun, Comparative adsorption isotherms and modeling of methylene blue onto activated carbons, Applied Water Science, 1 (2011) 111-117.

[60] M.J. Ahmed, S.K. Dhedan, Equilibrium isotherms and kinetics modeling of methylene blue adsorption on agricultural wastes-based activated carbons, Fluid Phase Equilibria, 317 (2012) 9-14.

[61] K. Vasanth Kumar, M.M. de Castro, M. Martinez-Escandell, M. Molina-Sabio, J. Silvestre-Albero, F. Rodriguez-Reinoso, A continuous site energy distribution function from Redlich–Peterson isotherm for adsorption on heterogeneous surfaces, Chemical Physics Letters, 492 (2010) 187-192.